ANTICANCER RESEARCH *37*: 6697-6703 (2017)
doi:10.21873/anticanres.12128

TP53 Mutation Status of Tubo-ovarian and Peritoneal High-grade Serous Carcinoma with a Wild-type p53 Immunostaining Pattern

KIYONG NA[1], JI-YOUN SUNG[2] and HYUN-SOO KIM[1]

[1]*Department of Pathology, Severance Hospital, Yonsei University College of Medicine, Seoul, Republic of Korea;*
[2]*Department of Pathology, Kyung Hee University School of Medicine, Seoul, Republic of Korea*

Abstract. *Background/Aim: Diffuse and strong nuclear p53 immunoreactivity and a complete lack of p53 expression are regarded as indicative of missense and nonsense mutations, respectively, of the TP53 gene. Tubo-ovarian and peritoneal high-grade serous carcinoma (HGSC) is characterized by aberrant p53 expression induced by a TP53 mutation. However, our experience with some HGSC cases with a wild-type p53 immunostaining pattern led us to comprehensively review previous cases and investigate the TP53 mutational status of the exceptional cases. Materials and Methods: We analyzed the immunophenotype of 153 cases of HGSC and performed TP53 gene sequencing analysis in those with a wild-type p53 immunostaining pattern. Results: Immunostaining revealed that 109 (71.3%) cases displayed diffuse and strong p53 expression (missense mutation pattern), while 39 (25.5%) had no p53 expression (nonsense mutation pattern). The remaining five cases of HGSC showed a wild-type p53 immunostaining pattern. Direct sequencing analysis revealed that three of these cases harbored nonsense TP53 mutations and two had novel splice site deletions. Conclusion: TP53 mutation is almost invariably present in HGSC, and p53 immunostaining can be used as a surrogate marker of TP53 mutation. In cases with a wild-type p53 immunostaining pattern, direct sequencing for TP53 mutational status can be helpful to confirm the presence of a TP53 mutation.*

Ovarian carcinoma is the most common cause of death from gynecological malignancies in developed countries. High-grade serous carcinoma (HGSC), the cause of 70% of ovarian carcinoma-related deaths, is typically diagnosed at advanced stages, when the tumors have already metastasized (1). The mainstay treatment for HGSC is debulking surgery followed by taxane-platinum combination chemotherapy (2). Despite improvements in surgical techniques as well as advances in chemotherapeutic agents, the majority of women with advanced-stage HGSC experience relapse within 2 years, ultimately develop chemoresistance, and succumb to their disease (2, 3).

The gene *TP53*, located on chromosome 17p13, encodes the tumor suppressor protein p53 (4). Mutations of *TP53* are the most common and most frequently studied genetic alterations in human malignancies (5). Wild-type p53 protein is relatively unstable and has a short half-life, which makes it undetectable by immunohistochemistry (5, 6). In contrast, mutant p53 has a much longer half-life and accumulates in the nucleus, creating a stable target for immunohistochemical detection (5). Diffuse and strong nuclear p53 immunoreactivity is regarded as indicative of a missense mutation of *TP53* (7-9). Furthermore, it has been shown that a complete lack of p53 expression is a result of a nonsense *TP53* mutation leading to formation of a truncated, non-immunoreactive protein (10-12). There is general agreement that aberrant (diffuse and strong or entirely absent) p53 expression is correlated with mutant p53, while expression levels between these two extremes are thought to represent wild-type p53 (2).

Tubo-ovarian and peritoneal HGSC are characterized by aberrant p53 expression induced by *TP53* mutation. In this regard, we currently use immunostaining patterns of p53 as a surrogate marker for *TP53* mutations in the diagnosis of tubo-ovarian and peritoneal HGSC. However, we experienced some cases of HGSC displaying a wild-type p53 immunostaining pattern, which initiated a comprehensive review of HGSC cases diagnosed at our Institution. In this study, we investigated the immunophenotype of tubo-ovarian and peritoneal HGSCs and performed *TP53* gene sequencing analysis to analyze *TP53* mutational status in HGSCs with a wild-type p53 immunostaining pattern.

Correspondence to: Hyun-Soo Kim, Department of Pathology, Severance Hospital, Yonsei University College of Medicine, 50-1, Yonsei-ro, Seodaemun-gu, Seoul 03722, Republic of Korea. Tel: +82 222281794, +82 23620860, e-mail: hyunsookim@yuhs.ac

Key Words: Ovary, high-grade serous carcinoma, p53, immunohistochemistry, *TP53* mutation, sequencing.

Table I. *Primer sequences used in this study.*

Primer name	Exon	Sequence	Size (bp)
TP53-ex-1_F	1	GTAAAACGACGGCCAGTGCTCAAGACTGGCGCTAAAA	225
TP53-ex-1_R		GCGGATAACAATTTCACACAGGGTGACTCAGAGAGGACTCAT	
TP53-ex-2_F	2	GTAAAACGACGGCCAGTGAAGCAGCCATTCTTTTCCT	454
TP53-ex-2_R		GCGGATAACAATTTCACACAGGGGTCCCCAGCCCAACCCTT	
TP53-ex-3_F	3	GTAAAACGACGGCCAGTGGAGCCGCAGTCAGATCCTA	274
TP53-ex-3_R		GCGGATAACAATTTCACACAGGGGTCCCCAGCCCAACCCTT	
TP53-ex-4_F	4	GTAAAACGACGGCCAGTCAACGTTCTGGTAAGGACAA	448
TP53-ex-4_R		GCGGATAACAATTTCACACAGGGCCAGGCATTGAAGTCTCAT	
TP53-ex-5_F	5	GTAAAACGACGGCCAGTGCCGTGTTCCAGTTGCTTTA	390
TP53-ex-5_R		GCGGATAACAATTTCACACAGGAGGAGGGGCCAGACCTAAGA	
TP53-ex-6_F	6	GTAAAACGACGGCCAGTAGCGCTGCTCAGATAGCGAT	350
TP53-ex-6_R		GCGGATAACAATTTCACACAGGTAAGCAGCAGGAGAAAGCCC	
TP53-ex-7_F	7	GTAAAACGACGGCCAGTAAGGCGCACTGGCCTCATCTT	305
TP53-ex-7_R		GCGGATAACAATTTCACACAGGGAGGTGGATGGGTAGTAG	
TP53-ex-8_F	8	GTAAAACGACGGCCAGTGACCTGATTTCCTTACTGCCT	258
TP53-ex-8_R		GCGGATAACAATTTCACACAGGTCTCCTCCACCGCTTCTT	
TP53-ex-9_F	9	GTAAAACGACGGCCAGTttgggagtagatggagcct	445
TP53-ex-9_R		GCGGATAACAATTTCACACAGGagtgttagactggaaacttt	
TP53-ex-10_F	10	GTAAAACGACGGCCAGTGGTACTTGAAGTGCAGTTTCT	383
TP53-ex-10_R		GCGGATAACAATTTCACACAGGCAGCTGCCTTTGACCATGAA	
TP53-ex-11_F	11	GTAAAACGACGGCCAGTCCAGCCTTAGGCCCTTCAAA	248
TP53-ex-11_R		GCGGATAACAATTTCACACAGGTGTCAGTGGGGAACAAGAA	

Materials and Methods

Case selection. This study (2017-1479-001) was reviewed and approved by the Institutional Review Board at Severance Hospital (Seoul, Republic of Korea). We selected 153 patients diagnosed with tubo-ovarian or peritoneal HGSC during the period from July 2015 to June 2016. Clinicopathological information was obtained from the electronic medical record system and pathology reports. Clinical and pathological details that were reviewed included age of patient at initial diagnosis, origin of tumor, association with serous tubal intraepithelial carcinoma (STIC), tubo-ovarian surface extension, presence of malignant cells in ascites or intraoperative peritoneal washings, pelvic or extrapelvic peritoneal metastasis, lymph node metastasis, lymphovascular invasion, and International Federation of Gynecology and Obstetrics (FIGO) stage.

Pathological examination. The tissues resected by gynecological oncology surgeons at Severance Hospital (Seoul, Republic of Korea) were initially examined by pathologists before fixation in 10% neutral-buffered formalin. After fixation for 12-24 h, the tissues were thoroughly examined macroscopically and sectioned. After processing with an automatic tissue processor (Peloris II; Leica Microsystems, Newcastle Upon Tyne, UK), the sections were embedded in paraffin blocks. Four micrometer-thick slices were cut from each formalin-fixed, paraffin-embedded tissue block using a rotary microtome (RM2245, Leica Microsystems) and stained with hematoxylin and eosin using an automatic staining instrument (Ventana Symphony System; Ventana Medical Systems, Tucson, AZ, USA). After staining, the slides were covered with a glass coverslip and sent to two Board-certified pathologists specialized in gynecological oncology (K.N. and H.-S.K.). They examined all available hematoxylin and eosin-stained slides by light microscopy (BX43 System Microscope; Olympus, Tokyo, Japan) and made definitive pathological diagnoses. In addition, the most representative slide for each case was chosen for immunohistochemical staining.

Immunohistochemical staining. Four micrometer-thick slices obtained from the formalin-fixed, paraffin-embedded tissue blocks were placed on Superfrost Plus glass slides (Thermo Fisher Scientific, Waltham, MA, USA). These slices were deparaffinized in xylenes and rehydrated through graded alcohols. Immunohistochemical staining was performed using automatic immunostaining instruments, either a Ventana Benchmark XT automated staining system (Ventana Medical Systems) or Dako Omnis system (Dako, Agilent Technologies, Carpinteria, CA, USA), according to the manufacturer's recommendations (13-17). Antigen retrieval was performed using Cell Conditioning Solution (CC1; Ventana Medical Systems) or EnVision FLEX Target Retrieval Solution, High pH (Dako, Agilent Technologies). The slices were incubated with primary antibody against paired box 8 (PAX8; 1:50, polyclonal; Cell Marque, Rocklin, CA, USA), Wilms tumor 1 (WT1; 1:200, clone 6F-H2; Cell Marque), p16 (prediluted, clone E6H4a; Ventana Medical Systems), p53 (1:300, clone DO-7; Novocastra, Leica Biosystems, Newcastle Upon Tyne, UK), estrogen receptor (ER; 1:150, clone 6F11; Novocastra), progesterone receptor (PR; 1:100; clone 16; Novocastra), hepatocyte nuclear factor 1β (HNF1β; 1:400, polyclonal; Sigma-Aldrich, St. Louis, MO, USA), and AT-rich interaction domain 1A (ARID1A; 1:400, polyclonal; Sigma-Aldrich). After chromogenic visualization using an ultraView Universal DAB Detection Kit (Ventana Medical Systems) or EnVision FLEX /HRP Kit (Dako, Agilent Technologies), the slices were counterstained with hematoxylin,

dehydrated in graded alcohols and xylene, and then embedded in mounting solution. Appropriate positive and negative controls were concurrently stained to validate the staining method. For negative controls, non-specific activity was assessed by omitting the primary antibodies. The p53 immunostaining pattern was interpreted as a missense mutation, nonsense mutation, or wild-type pattern when p53 expression was diffuse and strong (>60% of tumor cell nuclei), completely absent (0%), or focal and weakly positive, respectively.

Direct sequencing. Five cases of tubo-ovarian and peritoneal HGSC with a wild-type p53 immunostaining pattern were analyzed for *TP53* mutational status, as previously described (16). Briefly, histopathological confirmation for the presence of tumor tissue was performed by the two Board-certified pathologists. They marked the most dense tumor area on the hematoxylin and eosin-stained slides, avoiding necrotic and hemorrhagic areas as much as possible. Ten-micrometer-thick sections were cut from the formalin-fixed, paraffin-embedded tissue blocks. The areas that corresponded to the marked ones on the hematoxylin and eosin-stained slides were macrodissected with a scalpel and placed into 1.5-ml tubes for tissue digestion. Extraction of genomic deoxyribonucleic acid (DNA) was performed using a QIAamp DNA FFPE Mini Kit (Qiagen, Valencia, CA, USA). DNA concentrations of extracted DNA were determined using a NanoDrop ND-1000 spectrophotometer (Thermo Fisher Scientific) and adjusted to a concentration of 50 ng/μl. Exons 1-11 of *TP53* were amplified by polymerase chain reaction, using a DNA Engine Tetrad 2 Peltier Thermal Cycler (Bio-Rad Laboratories, Hercules, CA, USA). The primer sequences used are shown in Table I. Briefly, 50 ng of DNA was amplified with a thermal cycling profile of 95˚C for 5 min, 95˚C for 30 s, 60˚C for 30 s, 72˚C for 1 min, with a final extension at 72˚C for 7 min. Amplimers were purified using a Multiscreen Filter Plate (EMD Millipore, Billerica, MA, USA) and resolved by agarose gel electrophoresis to confirm successful amplification. Bidirectional Sanger sequencing of all polymerase chain reaction products was performed using a BigDye Terminator Version 3.1 Cycle Sequencing Kit (Applied Biosystems, Foster City, CA, USA). Sequence analysis was performed using an Applied Biosystems 3730xl Genetic Analyzer (Applied Biosystems) and Variant Reporter Software Version 1.1 (Applied Biosystems).

Table II. *Immunostaining results of 153 cases of tubo-ovarian and peritoneal high-grade serous carcinomas.*

Antibody	Immunostaining result	Number of cases (%)
PAX8	Positive/focally positive	153 (100.0)
	Negative	0 (0.0)
WT1	Positive/focally positive	151 (98.7)
	Negative	2 (1.3)
p53	Missense mutation pattern	109 (71.2)
	Nonsense mutation pattern	39 (25.5)
	Wild-type pattern	5 (3.3)
p16	Diffuse, strong positive	103 (69.1)
	Patchy positive	43 (28.9)
	Negative	3 (2.0)
	Not applicable	4
Estrogen receptor	Positive/Focally positive	97 (88.2)
	Negative	13 (11.8)
	Not applicable	43
Progesterone receptor	Positive/focally positive	24 (21.4)
	Negative	88 (78.6)
	Not applicable	41
HNF1β	Positive/focally positive (nuclear)	8 (18.2)
	Positive/focally positive (cytoplasmic)	11 (25.0)
	Positive/focally positive (membranous)	13 (29.5)
	Negative	12 (27.3)
	Not applicable	109
ARID1A	No loss	42 (100.0)
	Loss	0 (0.0)
	Not applicable	111

PAX8: Paired box 8; WT1: Wilms' tumor 1; HNF1β: hepatocyte nuclear factor 1β; ARID1A: AT-rich interaction domain 1A.

Results

Immunostaining results. Table II summarizes the immunostaining results of the 153 tubo-ovarian and peritoneal HGSCs. All (153/153; 100.0%) cases of HGSC examined were positive for PAX8. PAX8 expression was diffuse and strongly positive in 151/153 (98.7%) cases and focally positive in 2/153 (1.3%) cases. Similarly, WT1 expression was positive in 139/153 (90.8%) cases and focally positive in 12/153 (7.8%) cases. p53 immunostaining patterns corresponded with one of the following: diffuse and strong nuclear immunoreactivity (missense mutation pattern, 109/153; 71.2%), complete lack of expression (nonsense mutation pattern, 39/153; 25.5%), and scattered, weak-to-moderate nuclear immunoreactivity (wild-type pattern, 5/153; 3.3%). p16 expression was available in 151/153 cases; 103/151 (69.1%) cases were diffuse and strong positive for p16, while 43/151 (28.9%) cases showed patchy positive p16 expression. ER and PR were positive in 97/110 (88.2%) and 24/112 (21.4%) cases, respectively. The results of HNF1β and ARID1A immunostaining were available in 44/153 and 42/153 cases, respectively. Weak-to-moderate nuclear HNF1β immunoreactivity was observed in 8/44 (18.2%) cases. None of the 42 cases examined exhibited loss of ARID1A expression. Representative photomicrographs of immunohistochemical staining for PAX8, WT1, p53, p16, ER, PR, HNF1β, and ARID1A are shown in Figure 1.

Clinicopathological characteristics of five cases of tubo-ovarian and peritoneal high-grade serous carcinoma with a wild-type p53 immunostaining pattern. Table III summarizes the clinical and pathological characteristics of the five patients with tubo-ovarian and peritoneal HGSC with a wild-type p53 immunostaining pattern. The age at initial diagnosis ranged from 59 to 77 (median=68 years). One of the five cases was diagnosed with grade 2 HGSC, and the remaining four cases were grade 3. Tumors originated in the right ovary, left ovary, right fallopian tube, left fallopian tube, and peritoneum in one case each. STIC was detected in the right fimbria and left

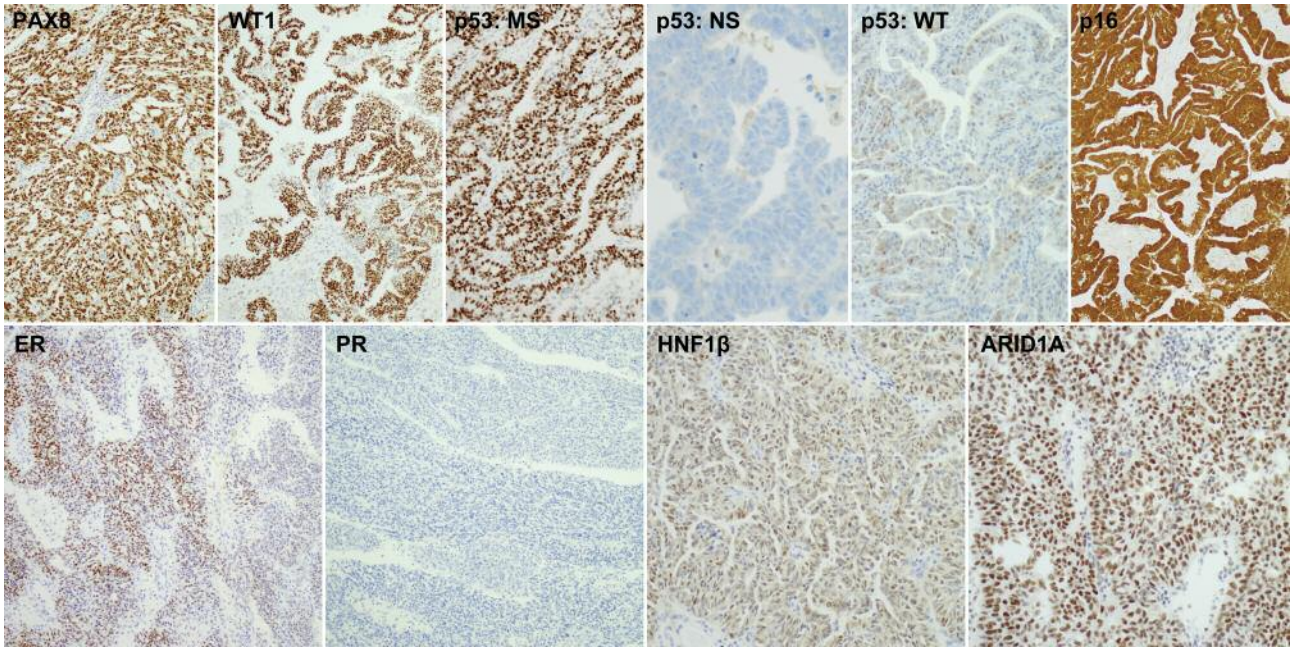

Figure 1. *Representative immunostaining results for high-grade serous carcinoma (HGSC). HGSC displays positive immunoreactivity for paired box 8 (PAX8), Wilms tumor 1 (WT1), and p16. p53 immunostaining patterns were classified as one of the following: missense (MS) mutation, nonsense (NS) mutation, and wild-type (WT). Most cases of HGSC exhibited estrogen receptor (ER) positivity and progesterone receptor (PR) negativity. Eight cases of HGSC displayed weak-to-moderate nuclear hepatocyte nuclear factor 1β (HNF1β) immunoreactivity. None of the HGSC cases examined showed loss of AT-rich interaction domain 1A (ARID1A) expression. Original magnification, PAX8, WT1, p16, ER, and PR, 100×; p53: MS, p53: WT, HNF1β, and ARID1A, 200×; p53: NS, 400×.*

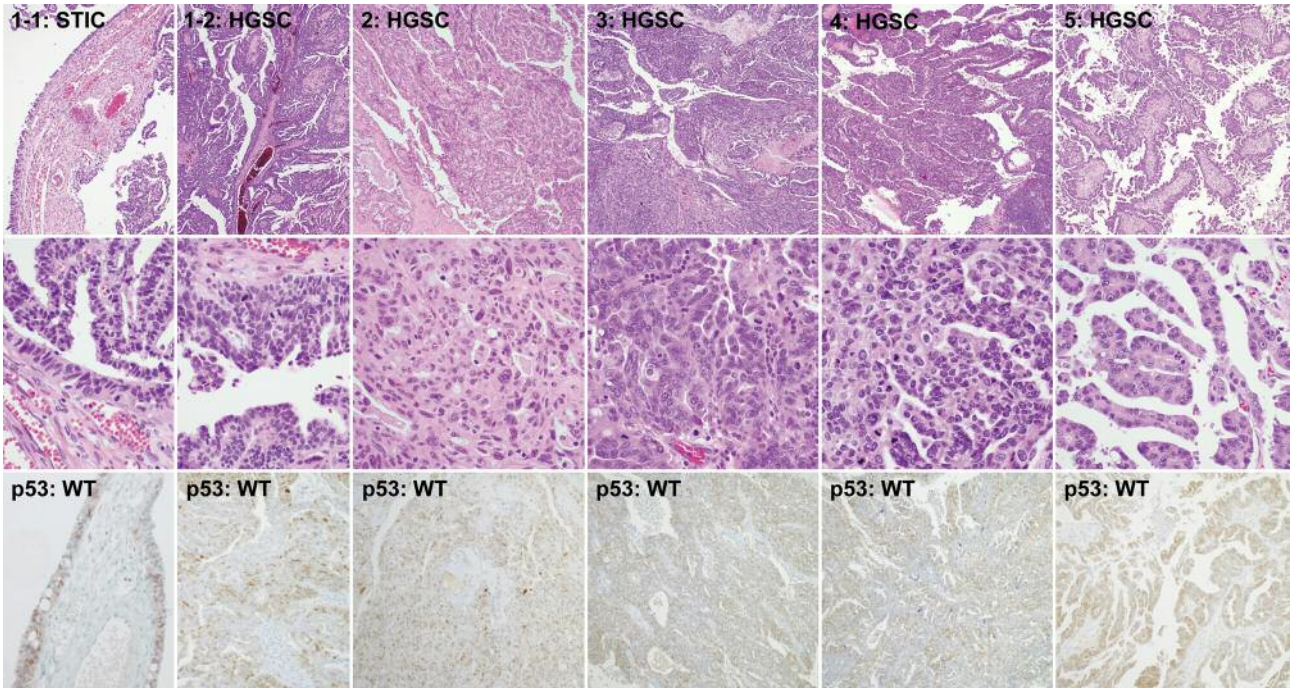

Figure 2. *Histopathological and immunohistochemical findings of high-grade serous carcinoma (HGSC) and serous tubal intraepithelial carcinoma (STIC) with a wild-type (WT) p53 immunostaining pattern in each sample (case and sample number shown). Both HGSCs and STIC displayed scattered, weak-to-moderate nuclear p53 immunoreactivity. Original magnification, upper panel, 40×; middle panel, 400×; lower panel, 40×.*

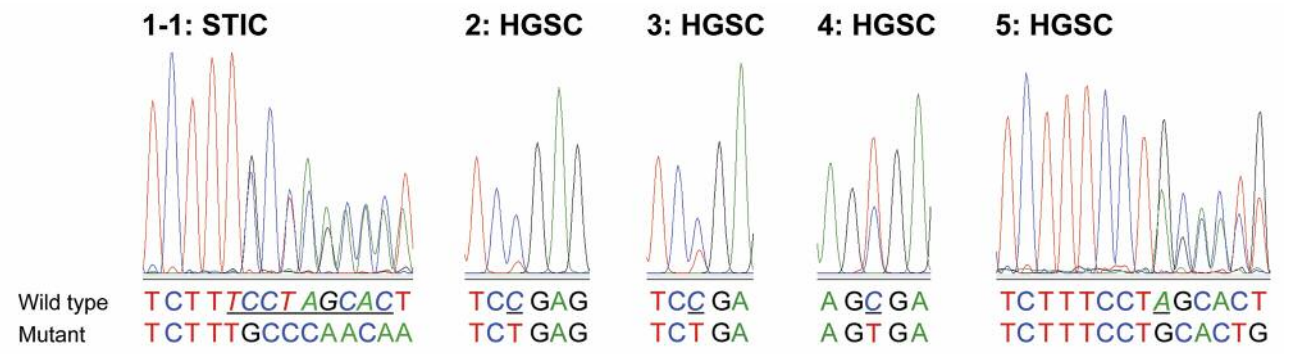

Figure 3. *Sequence chromatograms showing TP53 mutations in high-grade serous carcinoma (HGSC) and serous tubal intraepithelial carcinoma (STIC) with a wild-type p53 immunostaining pattern (case and sample number shown). Base changes in the sequence are italicized and underlined.*

Table III. *Clinicopathological characteristics of five cases of tubo-ovarian and peritoneal high-grade serous carcinoma with a wild-type p53 immunostaining pattern.*

Case	Age at initial Dx (years)	HGSC grade	Origin	STIC	Tubo-ovarian surface extension	Malignant cells in ascites or peritoneal washings	Peritoneal metastasis	LNM	LVI	FIGO stage
1	77	2	Right fallopian tube	Present	Present	Present	Pelvic/extrapelvic	Absent	Present	IVB
2	60	3	Left ovary	Absent	Absent	Present	Pelvic/extrapelvic	Absent	Absent	IVB
3	68	3	Right ovary	Absent	Present	Absent	Pelvic/extrapelvic	Absent	Absent	IIIB
4	59	3	Left fallopian tube	Present	Absent	Absent	Pelvic	Absent	Absent	IIB
5	72	3	Peritoneum	Absent	Present	Present	Pelvic/extrapelvic	Present	Present	IIIC

Dx: Diagnosis; FIGO: International Federation of Gynecology and Obstetrics; HGSC: high-grade serous carcinoma; LNM: lymph node metastasis; LVI: lymphovascular invasion; STIC: serous tubal intraepithelial carcinoma.

fimbria in one out of five cases each. The tumors involved the tubo-ovarian surfaces in three out of the five cases. Three out of the five patients had malignant tumor cells in the ascitic fluid or peritoneal fluid specimens collected intraoperatively. All patients underwent debulking surgery, consisting of total hysterectomy, bilateral salpingo-oophorectomy, pelvic and para-aortic lymph node dissection, total omentectomy, peritonectomy, and/or appendectomy. All patients had extrapelvic (4/5) or pelvic (5/5) peritoneal metastases at the time of diagnosis. Metastases to the pelvic and paraaortic lymph nodes were identified in one out of five patients. Tumor cell emboli within lymphatic and vascular spaces were detected in three out of five cases. FIGO stage of the patients was IIB, IIIB, and IIIC in one case each, and IVB in two.

TP53 mutational status of five cases of tubo-ovarian and peritoneal high-grade serous carcinoma with a wild-type p53 immunostaining pattern. Table IV summarizes the sequencing results of the five tubo-ovarian and peritoneal HGSCs with a wild-type p53 immunostaining pattern. Three out of the seven samples were collected from the right fallopian tube (STIC), left ovary (HGSC), and omentum (HGSC) of a single patient. Each of the remaining four samples was obtained from a single patient. All seven samples examined harbored *TP53* mutations. Three out of the seven samples (cases 2, 3, and 4) harbored nonsense mutations in exon 8 [NM_000546.5:c.916C>T (p.R306*); 1/7] or exon 10 [NM_000546.5:c.1024C>T (p.342*); 2/7]. In the remaining four samples, novel deletion mutations affecting the splice site were identified in intron 8 [NM_000546.5:c.920-6_922delTCCTAGCAC (3/7; case 1) and NM_000546.5:c.920-2delA (1/7; case 5)]. The chromatographs of the analyzed sequences are shown in Figure 3. The following single nucleotide polymorphisms were also detected: NM_000546.5:c.74+38C>G (rs1642785) and NM_000546.5:c.215C>G (rs1042522; 7/7) in all seven samples; NM_000546.5:c.672+62A>G (rs1625895) in three samples; NM_000546.5:c.97-29C>A (rs17883323) in two

Table IV. *TP53 mutational status of five cases of tubo-ovarian and peritoneal high-grade serous carcinoma with a wild-type p53 immunostaining pattern.*

Case	Sample	*TP53* mutation		
		Region	DNA sequence change	Predicted effect
1	1-1: STIC, right fallopian tube	i8-intron	c.920-6_922delTCCTAGCAC	Splice site deletion
	1-2: HGSC, left ovary	i8-intron	c.920-6_922delTCCTAGCAC	Splice site deletion
	1-3: HGSC, omentum	i8-intron	c.920-6_922delTCCTAGCAC	Splice site deletion
2	2: HGSC, left ovary	10-exon	c.1024C>T	p.R342*
3	3: HGSC, posterior cul-de-sac	10-exon	c.1024C>T	p.R342*
4	4: HGSC, left ovary	8-exon	c.916C>T	p.R306*
5	5: HGSC, cul-de-sac	i8-intron	c.920-2delA	Splice site deletion

HGSC: High-grade serous carcinoma; STIC: serous tubal intraepithelial carcinoma.

samples; and NM_000546.5:c.108G>A (rs1800370), NM_000546.5:c.782+72C>T (rs12947788), and NM_000 546.5:c.782+92T>G (rs12951053) in one sample each.

Discussion

According to the World Health Organization Classification of Tumors of Female Reproductive Organs revised in 2014 (18), the rates of positivity for PAX8, WT1, ER, and PR in HGSC were 98%, 92%, 80%, and 30%, respectively. The frequencies of aberrant expression of p53 and p16 were 93% and 60%, respectively. These data were comparable to our results showing positivity for PAX8, WT1, ER, and PR in 100.0%, 98.7%, 88.2%, and 21.4% of HGSCs, respectively, and the aberrant expression of p53 and p16 in 96.7% and 69.1% of cases examined, respectively.

TP53 mutations are pervasive in tubo-ovarian and peritoneal HGSC, occurring in 70-95% of HGSCs (2, 5). Yemelyanova *et al*. showed that immunohistochemical analysis correlated with *TP53* mutational analysis in 94.4% of HGSC cases based on the combination of p53 overexpression (>60%) and complete lack of p53 expression (0%) (5). Another study using similar cut-off values (>70% for overexpression and <5% for lack of expression) showed matched results between immunostaining and mutational analyses in 95.8% of HGSC cases (2). In this study, the mutation pattern of p53 immunostaining was found in 96.7% cases when cut-off values of >60% for overexpression and 0% for lack of expression were used (18). Although false-positive staining can occur, it generally affects only a few cases.

Patchy p53 expression (wild-type p53 immunostaining pattern) may indicate either wild-type *TP53* or, rarely, false-negative results. False-negative p53 staining was reported by others in 1/72 and 2/57 cases harboring nonsense and missense *TP53* mutations, respectively (2, 5). In this study, five cases exhibited a wild-type p53 immunostaining pattern. Using direct sequencing, we found that three out of five cases harbored known nonsense mutations, indicating false-negative results in p53 immunostaining. Patchy p53 expression observed in cases harboring nonsense *TP53* mutation may be explained by delayed degradation of the truncated protein. It has been suggested that cellular stress may delay degradation of p53, allowing it to be detected on immunohistochemistry (19). Wild-type p53 sequestered within the cytoplasm is resistant to mouse double minute 2 homolog-mediated degradation. Intratumoral heterogeneity may also account for the discrepancy (18); tumors can acquire *TP53* mutation as a late event. Although *TP53* mutation has been known to be a dominant driver mutation in tubo-ovarian and peritoneal HGSC, wild-type *TP53* in a small subset of HGSCs implies that other genetic alterations may play a crucial role in carcinogenesis (2).

We also found splice site deletions in two out of five cases with a wild-type p53 immunostaining pattern. In a previous study, splice site mutations were detected in 5/72 HGSCs, and other genetic mutations were not found in these tumors, indicating that the splice site mutation is related to the development of tubo-ovarian HGSC (2). Splice site mutations identical to those we observed have been reported in pulmonary squamous cell carcinoma (20) and Li-Fraumeni syndrome (20, 21). Stecher *et al*. (21) observed multiple longer splicing products in samples obtained from Li-Fraumeni syndrome patients carrying splice site mutations. Although splice site mutations of *TP53* are relatively infrequent in HGSC and their effects have not been well characterized, the novel splice site deletion mutations (NM_000546.5:c.920-6_922delTCCTAGCAC and NM_000546.5:c.920-2delA) observed in this study are thought to be involved in the pathogenesis of HGSC (21-23).

In summary, we investigated the immunophenotype of tubo-ovarian and peritoneal HGSC and found five cases with a wild-type p53 immunostaining pattern. Direct sequencing

analysis revealed nonsense *TP53* mutations in three of these cases and novel splice site deletions in the other two. Our results support the notion that *TP53* mutation is almost invariably present in HGSC and that p53 immunostaining can be used as a surrogate marker of *TP53* mutation. In cases with a wild-type p53 immunostaining pattern, direct sequencing for *TP53* mutational status can be helpful in confirming the presence of a *TP53* mutation.

Acknowledgements

This research was supported by the Basic Science Research Program through the National Research Foundation of Korea (NRF) funded by the Ministry of Science, ICT & Future Planning (2017R1A2B4007704) and by the Ministry of Education (2016R1D1A1B03935584).

References

1 Kim J, Coffey DM, Creighton CJ, Yu Z, Hawkins SM and Matzuk MM: High-grade serous ovarian cancer arises from fallopian tube in a mouse model. Proc Natl Acad Sci USA *109*: 3921-3926, 2012.

2 Cole AJ, Dwight T, Gill AJ, Dickson KA, Zhu Y, Clarkson A, Gard GB, Maidens J, Valmadre S, Clifton-Bligh R and Marsh DJ: Assessing mutant p53 in primary high-grade serous ovarian cancer using immunohistochemistry and massively parallel sequencing. Sci Rep *6*: 26191, 2016.

3 Bukowski RM, Ozols RF and Markman M: The management of recurrent ovarian cancer. Semin Oncol *34*: S1-15, 2007.

4 Ahmed AA, Etemadmoghadam D, Temple J, Lynch AG, Riad M, Sharma R, Stewart C, Fereday S, Caldas C, Defazio A, Bowtell D and Brenton JD: Driver mutations in TP53 are ubiquitous in high grade serous carcinoma of the ovary. J Pathol *221*: 49-56, 2010.

5 Yemelyanova A, Vang R, Kshirsagar M, Lu D, Marks MA, Shih Ie M and Kurman RJ: Immunohistochemical staining patterns of p53 can serve as a surrogate marker for *TP53* mutations in ovarian carcinoma: an immunohistochemical and nucleotide sequencing analysis. Mod Pathol *24*: 1248-1253, 2011.

6 Rogel A, Popliker M, Webb CG and Oren M: p53 cellular tumor antigen: analysis of mRNA levels in normal adult tissues, embryos, and tumors. Mol Cell Biol *5*: 2851-2855, 1985.

7 Bartek J, Iggo R, Gannon J and Lane DP: Genetic and immunochemical analysis of mutant p53 in human breast cancer cell lines. Oncogene *5*: 893-899, 1990.

8 Bennett WP, Hollstein MC, Hsu IC, Sidransky D, Lane DP, Vogelstein B and Harris CC: Mutational spectra and immunohistochemical analyses of p53 in human cancers. Chest *101*: 19S-20S, 1992.

9 Iggo R, Gatter K, Bartek J, Lane D and Harris AL: Increased expression of mutant forms of *p53* oncogene in primary lung cancer. Lancet *335*: 675-679, 1990.

10 Lax SF, Kendall B, Tashiro H, Slebos RJ and Hedrick L: The frequency of *p53*, *K-ras* mutations, and microsatellite instability differs in uterine endometrioid and serous carcinoma: evidence of distinct molecular genetic pathways. Cancer *88*: 814-824, 2000.

11 Shahin MS, Hughes JH, Sood AK and Buller RE: The prognostic significance of p53 tumor suppressor gene alterations in ovarian carcinoma. Cancer *89*: 2006-2017, 2000.

12 Tashiro H, Isacson C, Levine R, Kurman RJ, Cho KR and Hedrick L: *p53* gene mutations are common in uterine serous carcinoma and occur early in their pathogenesis. Am J Pathol *150*: 177-185, 1997.

13 Do SI, Yoon G, Kim HS, Kim K, Lee H, Do IG, Kim DH, Chae SW and Sohn JH: Increased brahma-related gene 1 expression predicts distant metastasis and shorter survival in patients with invasive ductal carcinoma of the breast. Anticancer Res *36*: 4873-4882, 2016.

14 Jang MI, Sung JY, Kim JY and Kim HS: Clinicopathological characteristics of metaplastic papillary tumor of the fallopian tube. Anticancer Res *37*: 3693-3701, 2017.

15 Kim JY, Na K and Kim HS: Clinicopathological characteristics of mitotically-active cellular fibroma of the ovary: a single-institutional experience. Anticancer Res *37*: 2557-2564, 2017.

16 Na K, Kim EK, Jang W and Kim HS: *CTNNB1* mutations in ovarian microcystic stromal tumors: identification of a novel deletion mutation and the use of pyrosequencing to identify reported point mutation. Anticancer Res *37*: 3249-3258, 2017.

17 Na K, Sung JY and Kim HS: Stromal p16 overexpression in adult granulosa cell tumors of the ovary. Anticancer Res *37*: 2437-2444, 2017.

18 Mota A, Trivino JC, Rojo-Sebastian A, Martinez-Ramirez A, Chiva L, Gonzalez-Martin A, Garcia JF, Garcia-Sanz P and Moreno-Bueno G: Intra-tumor heterogeneity in *TP53* null high grade serous ovarian carcinoma progression. BMC Cancer *15*: 940, 2015.

19 Zaika A, Marchenko N and Moll UM: Cytoplasmically "sequestered" wild type p53 protein is resistant to MDM2-mediated degradation. J Biol Chem *274*: 27474-27480, 1999.

20 Lee EB, Jin G, Lee SY, Park JY, Kim MJ, Choi JE, Jeon HS, Cha SI, Cho S, Kim CH, Park TI, Jung TH, Son JW and Park JY: *TP53* mutations in Korean patients with non-small cell lung cancer. J Korean Med Sci *25*: 698-705, 2010.

21 Stecher CW, Gronbaek K and Hasle H: A novel splice mutation in the *TP53* gene associated with Leydig cell tumor and primitive neuroectodermal tumor. Pediatr Blood Cancer *50*: 701-703, 2008.

22 Fleury H, Communal L, Carmona E, Portelance L, Arcand SL, Rahimi K, Tonin PN, Provencher D and Mes-Masson AM: Novel high-grade serous epithelial ovarian cancer cell lines that reflect the molecular diversity of both the sporadic and hereditary disease. Genes Cancer *6*: 378-398, 2015.

23 Wojnarowicz PM, Oros KK, Quinn MC, Arcand SL, Gambaro K, Madore J, Birch AH, de Ladurantaye M, Rahimi K, Provencher DM, Mes-Masson AM, Greenwood CM and Tonin PN: The genomic landscape of TP53 and p53 annotated high-grade ovarian serous carcinomas from a defined founder population associated with patient outcome. PLoS One *7*: e45484, 2012.

Received September 5, 2017
Revised September 22, 2017
Accepted September 27, 2017